

## Multicolor vortex solitons in two-dimensional photonic lattices

Zhiyong Xu,<sup>1</sup> Yaroslav V. Kartashov,<sup>1,2</sup> Lucian-Cornel Crasovan,<sup>1,3</sup> Dumitru Mihalache,<sup>3</sup> and Lluís Torner<sup>1</sup>

<sup>1</sup>*ICFO-Institut de Ciències Fòtoniques, and Department of Signal Theory and Communications, Universitat Politècnica de Catalunya, 08034 Barcelona, Spain*

<sup>2</sup>*Physics Department, M. V. Lomonosov Moscow State University, 119899 Moscow, Russia*

<sup>3</sup>*Institute of Atomic Physics, Department of Theoretical Physics, P.O. Box MG-6, Bucharest, Romania*

(Received 7 September 2004; published 27 January 2005)

We report on the existence and stability of multicolor lattice vortex solitons constituted by coupled fundamental frequency and second-harmonic waves in optical lattices in quadratic nonlinear media. It is shown that the solitons are stable almost in the entire domain of their existence, and that the instability domain decreases with the increase of the lattice depth. We also show the generation of the solitons, and the feasibility of the concept of *lattice soliton algebra*.

DOI: 10.1103/PhysRevE.71.016616

PACS number(s): 42.65.Tg, 42.65.Wi, 42.79.Gn

Localized structures, especially solitons, play a crucial role in many branches of nonlinear science. Over the past several decades, the existence and unique properties of spatial, temporal, and spatiotemporal optical solitons in homogeneous cubic and quadratic nonlinear media have been studied both theoretically and experimentally (for detailed reviews, see Refs. [1–3]). Solitons arise as a result of the balance between linear diffracting and/or dispersing properties of the medium and a nonlinear mechanism responsible for focusing/defocusing. One important subject of study is the generation of nonlinear modes with a nontrivial phase, such as vortices. In optics, vortices are associated with screw phase dislocations nested in light beams [4]. Here we are interested in vortices with a bright shape, i.e., dislocations nested in finite-size beams [5]. In homogeneous pure cubic and quadratic uniform media such ring-shaped vortex solitons suffer azimuthal instabilities which have been observed experimentally in different settings [6]. They can be made stable in media with competing nonlinearities [7], and in media with refractive index modulations that we address here.

Propagation of optical radiation in media with transverse refractive index modulation differs considerably from the propagation in uniform media. Localized structures in such periodic media, termed discrete or lattice solitons, do exist and exhibit a rich variety of topologies. Since the theoretical prediction of discrete optical solitons in 1988 [8] they keep attracting a growing interest, in part because of their potential for all-optical switching and routing phenomena [9–11]. The intermediate regime between continuous and discrete solitons [12,13], constituted by continuous nonlinear media with an imprinted transverse modulation of the refractive index, has been shown recently to offer a variety of new opportunities. The concept behind this regime might be termed *tunable discreteness*, with the strength of modulation being the parameter that tunes the system properties from predominantly continuous to predominantly discrete. In this context, wave dynamics is governed by the interplay between optical tunnelling to adjacent sites and nonlinearity. This kind of lattice solitons has been observed recently in two-dimensional (2D) photorefractive optical lattices [14–18].

Besides the study of the existence and stability properties of fundamental (ground state) modes in the nonlinear media with periodic potentials an intriguing question is whether the action of the confining potential can permit the formation of vorticity carrying localized structures. Theoretical works showed that such complex localized structures, i.e., *lattice vortex solitons* exist when an optical lattice acts on a Kerr or photorefractive nonlinear crystal [19–21]. Recently, theoretical expectations were indeed confirmed experimentally by two independent groups [22,23]. During the last years various families of solitons in arrays of weakly coupled waveguides made with quadratic nonlinear media have been investigated [24–29] and observed [30]. One-dimensional (1D) multicolor solitons in lattices with tunable strength have been also studied recently, and their potential applications for packing and steering single solitons have been investigated [31]. Two-dimensional geometries might support even robust soliton ensembles with phase dislocations, the problem that we address in this work.

We thus report on the existence and stability of such multicolor lattice vortex solitons, which comprise four main humps arranged in a square configuration. It is shown that the lattice vortex solitons are stable almost in the entire domain of their existence except for a narrow region near the cutoff, and that the instability domain decreases with the increase of the lattice depth. We also investigate the possibility of their dynamical generation [32] from Gaussian-type input beams with nested vorticities.

We study the system of coupled nonlinear equations that describe the interaction between the fundamental frequency (FF) and second-harmonic (SH) waves under conditions for type-I second-harmonic generation in bulk materials in the absence of Poynting vector walkoff:

$$i \frac{\partial q_1}{\partial \xi} = \frac{d_1}{2} \left( \frac{\partial^2 q_1}{\partial \eta^2} + \frac{\partial^2 q_1}{\partial \zeta^2} \right) - q_1^* q_2 \exp(-i\beta\xi) - pR(\eta, \zeta) q_1,$$

$$i \frac{\partial q_2}{\partial \xi} = \frac{d_2}{2} \left( \frac{\partial^2 q_2}{\partial \eta^2} + \frac{\partial^2 q_2}{\partial \zeta^2} \right) - q_1^2 \exp(i\beta\xi) - 2pR(\eta, \zeta) q_2, \quad (1)$$

where  $q_1 = (2k_1/k_2)^{1/2} [2\pi\omega_0^2\chi^{(2)}r_0^2/c^2] A_1$  and  $q_2 = [2\pi\omega_0^2\chi^{(2)}r_0^2/c^2] A_2$  represent the normalized complex am-

plitudes of the FF and SH fields,  $k_1=k(\omega_0)$ ,  $k_2=k(2\omega_0) \approx 2k_1$ ,  $r_0$  is the transverse scale of the input beams,  $\eta = x/r_0$ ,  $\zeta = y/r_0$ ,  $\xi = z/(k_1 r_0^2)$ ,  $\beta = (2k_1 - k_2)k_1 r_0^2$  is the phase mismatch,  $d_1 = -1$ ,  $d_2 = -k_1/k_2 \approx -1/2$ , and  $p = 2\pi\omega_0^2 \delta\chi^{(1)} r_0^2 / c^2$  is the lattice depth. The function  $R(\eta, \zeta) = \cos(2\pi\eta/T)\cos(2\pi\zeta/T)$  describes the transverse refractive index profile, where  $T$  is the modulation period. The system (1) admits several conserved quantities, including the energy flow

$$U = \int \int_{-\infty}^{+\infty} (|q_1|^2 + |q_2|^2) d\eta d\zeta, \quad (2)$$

and the Hamiltonian

$$H = \int \int_{-\infty}^{+\infty} \left[ -\frac{d_1}{2} |\nabla q_1|^2 - \frac{d_2}{4} |\nabla q_2|^2 - \frac{1}{2} (q_1^*)^2 q_2 \exp(-i\beta\xi) - \frac{1}{2} q_1^2 q_2^* \exp(i\beta\xi) + \frac{\beta}{2} |q_2|^2 - pR(\eta, \zeta) |q_1|^2 - pR(\eta, \zeta) |q_2|^2 \right] d\eta d\zeta, \quad (3)$$

where  $\nabla = \mathbf{e}_\eta (\partial/\partial\eta) + \mathbf{e}_\zeta (\partial/\partial\zeta)$ , and  $\mathbf{e}_\eta$ ,  $\mathbf{e}_\zeta$  are unity vectors along  $\eta$  and  $\zeta$  axes.

We searched for the stationary solutions in the form  $q_1 = [u_1(\eta, \zeta) + iv_1(\eta, \zeta)] \exp(ib_1\xi)$  and  $q_2 = [u_2(\eta, \zeta) + iv_2(\eta, \zeta)] \exp(ib_2\xi)$ , where  $u_{1,2}(\eta, \zeta)$  and  $v_{1,2}(\eta, \zeta)$  are real functions, and  $b_{1,2}$  are real propagation constants that verify  $b_2 = \beta + 2b_1$ . Substitution of the above expressions into Eq. (1) yields the following system of equations for the soliton profiles  $u_{1,2}$  and  $v_{1,2}$

$$\begin{aligned} \frac{d_1}{2} \left( \frac{\partial^2 u_1}{\partial \eta^2} + \frac{\partial^2 u_1}{\partial \zeta^2} \right) - u_1 u_2 - v_1 v_2 + b_1 u_1 - pR(\eta, \zeta) u_1 &= 0, \\ \frac{d_1}{2} \left( \frac{\partial^2 v_1}{\partial \eta^2} + \frac{\partial^2 v_1}{\partial \zeta^2} \right) - u_1 v_2 + v_1 u_2 + b_1 v_1 - pR(\eta, \zeta) v_1 &= 0, \\ \frac{d_2}{2} \left( \frac{\partial^2 u_2}{\partial \eta^2} + \frac{\partial^2 u_2}{\partial \zeta^2} \right) - u_1^2 + v_1^2 + b_2 u_2 - 2pR(\eta, \zeta) u_2 &= 0, \\ \frac{d_2}{2} \left( \frac{\partial^2 v_2}{\partial \eta^2} + \frac{\partial^2 v_2}{\partial \zeta^2} \right) - 2u_1 v_1 + b_2 v_2 - 2pR(\eta, \zeta) v_2 &= 0. \end{aligned} \quad (4)$$

We solved the system of coupled equations (4) numerically by using a standard relaxation method. The lattice vortex soliton families are one-parameter families defined by the propagation constant  $b_1$  for any given period of the modulation  $T$ , lattice depth  $p$ , and phase mismatch  $\beta$ . Since one can use scaling transformations  $q_{1,2}(\eta, \zeta, \xi, \beta, p) \rightarrow \chi^2 q_{1,2}(\chi\eta, \chi\zeta, \chi^2\xi, \chi^2\beta, \chi^2p)$  to obtain various families of solitons from a given family, we have selected the transverse scale  $r_0$  such that the modulation period is given by  $T = \pi/2$  and then we have varied  $b_1$ ,  $\beta$ , and  $p$ .

The simplest vortex soliton with unit topological charge in two-dimensional periodic lattice is shown in Fig. 1. It comprises four main humps arranged in a square configura-

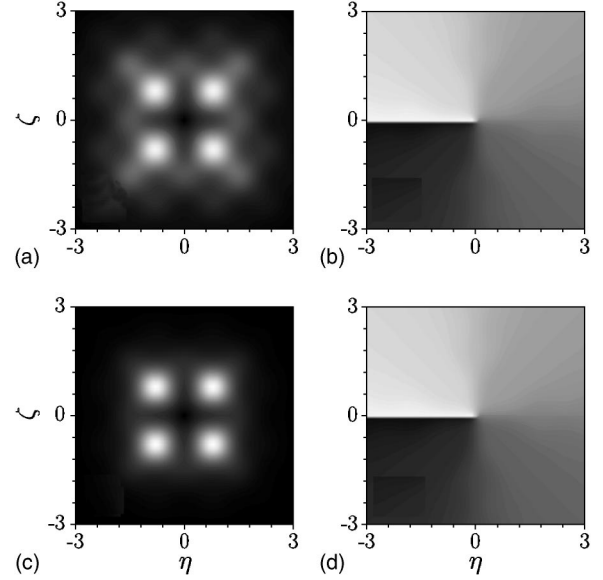


FIG. 1. (a) Profile and (b) phase of vortex solitons supported by the harmonic lattice at  $b_1=1.07$ . (c) Profile and (d) phase of vortex soliton at  $b_1=2$ . Only the FF wave is shown. Lattice depth  $p=4$ , phase mismatch  $\beta=0$ .

tion with a stairlike phase structure that is topologically equivalent to the phase of a conventional vortex in uniform medium [see Figs. 1(b) and 1(d)]. The positions of the soliton intensity maxima almost coincide with the positions of the local maxima of the lattice. Note that the singularity of these vortex solitons is centered between four lattice sites, that is they belong to the class of the, so called, *off-site* vortex soliton. In the model we investigated here there exist also a family of *on-site* vortex solitons (not shown here). In that case the phase singularity is centered on a lattice site [20,22,23]. We will restrict ourselves here to the case of the off-site vortex solitons. It is interesting to note that these stationary structures somehow resembles the four-soliton molecules carrying orbital angular momentum that were investigated in a variety of nonlinear media in both two-dimensional and three-dimensional geometries [33–35]. The typical stairlike phase distribution in the case of the above mentioned soliton molecules is clearly seen in panels (b) and (d) of Fig. 1 for the lattice vortex solitons. We want to mention that the 1D quadratic waveguides were also shown to support various families of multi-peaked solitons, which display combinations of in-phase and out-of-phase odd solitons, the latter ones with  $\pi$  phase jumps between neighbor solitons [31].

It should be noted that at low powers (small  $b_1$ ) the lattice vortex solitons are quite wide and spread out over many lattice sites [Fig. 1(a)], while at high powers the energy is mainly localized within the corresponding four peaks [Fig. 1(c)]. We did not find four-hump structures with higher topological charges (two or more), and all other higher-order stationary structures we have found (for example, lattice vortex solitons with eight humps) were found to be unstable on propagation. Thus in this work we will restrict ourselves to the study of the properties of simplest four-hump lattice vortex solitons.

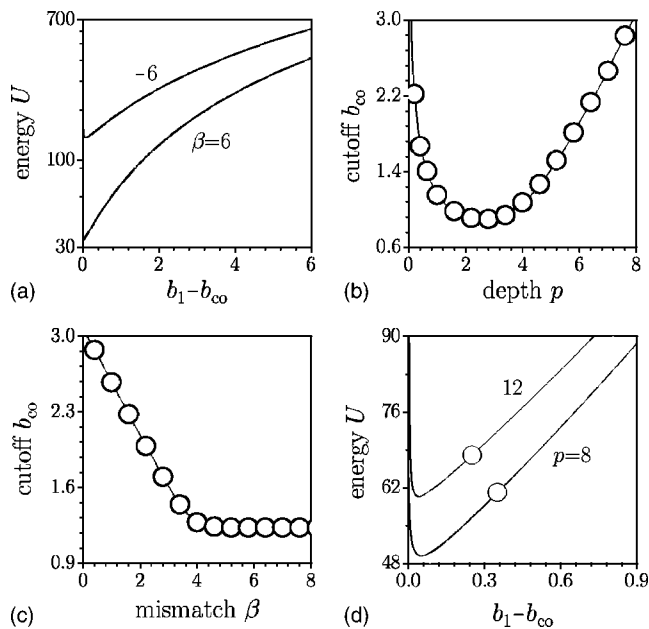


FIG. 2. (a) Vortex soliton energy flow versus propagation constant for different values of phase mismatch at  $p=8$ . (b) Propagation constant cutoff versus lattice depth at  $\beta=0$ . (c) Cutoff versus phase mismatch at  $p=8$ . (d) Stability and instability domains for different lattice depths at  $\beta=0$ . Circles show critical value of propagation constant for stabilization.

In order to characterize the families of lattice vortex solitons we have calculated the energy flows associated with these stationary solutions as well as their existence domains for given lattice depth  $p$  and phase mismatch  $\beta$ . As a general rule, the energy flow of the four-hump lattice vortex solitons is a nonmonotonic function of the propagation constant [even if this cannot be seen directly from Fig. 2(d) without zooming]. Note that in Figs. 2(a) and 2(d) on the abscissa we have plotted the difference  $(b_1 - b_{co})$  between the propagation constant  $b_1$  and cutoff value  $b_{co}$ . The cutoff value depends on both the phase mismatch  $\beta$  and lattice depth  $p$ . For example at  $p=8$  cutoff is given by  $b_{co}=6.065$  for  $\beta=-6$ , while  $b_{co}=1.23$  for  $\beta=6$ . The cutoff  $b_{co}$  is a nonmonotonic function of the lattice depth  $p$  [Fig. 2(b)]. It tends to infinity at  $p \rightarrow 0$  and  $p \rightarrow +\infty$ . One can see from Fig. 2(c) that in the presence of the lattice the dependence  $b_{co}(\beta)$  differs from that for quadratic solitons in continuous media:  $b_{co}(\beta) = \max\{-\beta/2, 0\}$ . Thus at  $\beta \rightarrow -\infty$  cutoff is approximately given by  $(\beta - \beta_0)/2$ , while at  $\beta \rightarrow +\infty$  one has  $b_{co} = b_0$ , where  $\beta_0$  is the mismatch shift due to the lattice. Both  $b_0$  and  $\beta_0$  growth with  $p$ . This property holds also for the one-dimensional lattice solitons in quadratic nonlinear media [31].

The periodic refractive index modulation affects also the energy sharing between FF and SH waves. For example, at a given phase mismatch  $\beta$ , the fraction of the total energy flow carried by the SH wave increases with increase of the lattice depth. Moreover, near the cutoff, the SH wave spreads over more lattice sites than the FF beam. As in the case of a uniform media, in the lattice with fixed depth  $p$  the part of energy flow carried by the SH wave decreases with increase of phase mismatch  $\beta$ .

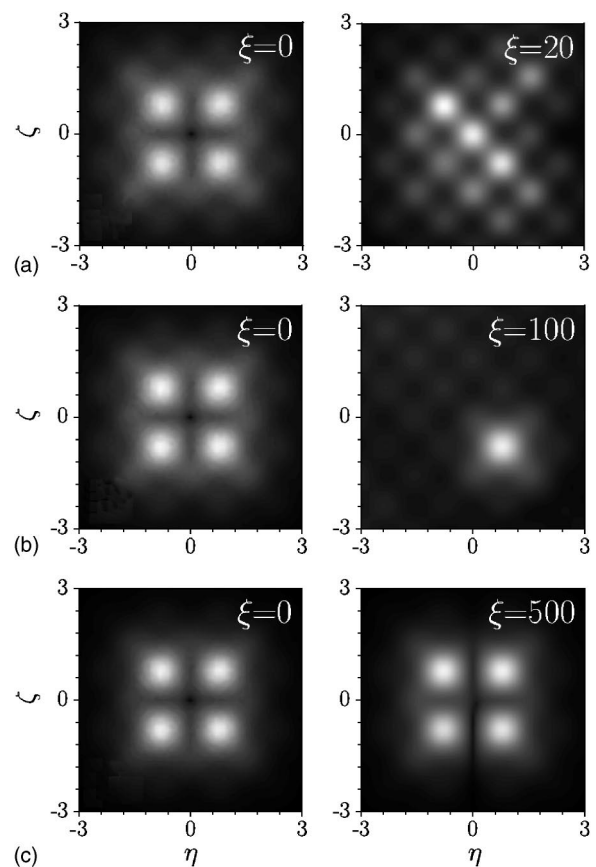


FIG. 3. Propagation of vortex solitons with  $b_1=3.1$  (a), 3.4 (b), and 5 (c) in the presence of input noise with variance  $\sigma_{noise}^2=0.01$ . FF wave profile is shown at different propagation distances. Lattice depth  $p=8$ , phase mismatch  $\beta=0$ .

To investigate the stability of the lattice vortex solitons, we have performed extensive numerical simulations of the evolution dictated by Eq. (1) with the input conditions  $q_1(\xi=0)=[u_1(\eta, \zeta) + iv_1(\eta, \zeta)][1 + \rho_1(\eta, \zeta)]$  and  $q_2(\xi=0)=[u_2(\eta, \zeta) + iv_2(\eta, \zeta)][1 + \rho_2(\eta, \zeta)]$ , where  $u_{1,2}$  and  $v_{1,2}$  are the exact solutions of Eq. (4) and  $\rho_{1,2}$  are random functions with Gaussian distribution and variance  $\sigma_{noise}^2=0.01$ . We have propagated the perturbed four-hump lattice vortex solitons over thousands of units for various values of the physical parameters involved  $(\beta, p, U)$ .

Our simulations show that there exists a narrow instability band near the propagation constant cutoff  $b_{co}$  for vortex solitons, but above a certain critical value of propagation constant they appear to become free of instability. We have found that the width of instability domain of lattice vortex solitons decreases with increase of the depth of the lattice  $p$  [Fig. 2(d)]. For example, as depicted in Fig. 2(d), the width of instability domain on propagation constant for  $p=12$  is approximately given by 0.24, while for  $p=8$  it is 0.35.

A few representative decay scenarios for the unstable four-hump lattice vortex solitons with unit topological charge are shown in Fig. 3. In the row (a) of Fig. 3 we show the typical decay of the unstable vortex soliton in the vicinity of the cutoff on propagation constant  $b_{co}$ . The initial energy of the localized structure is spreading out during evolution across the whole lattice and the vortex soliton disappears.

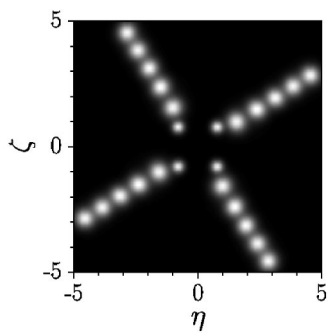


FIG. 4. Snapshot images showing decay of the stable vortex solitons caused by removal of the lattice. Only SH wave profile is shown. Images are taken after each 2.5 propagation units. Lattice depth  $p=8$ , phase mismatch  $\beta=0$ .

Notice that this type of instability develops exponentially. In the rest part of the instability domain located closer to critical value of the propagation constant, we encountered oscillatory-type instability. Upon development of this instability vortex soliton transforms into a fundamental (ground state) lattice soliton that is the most robust and energetically stable state of the system [see row (b) of Fig. 3], through increasing oscillations of four intensity maxima of the vortex.

One of the important results of this study is that the lattice vortex soliton becomes completely stable when its propagation constant exceeds a critical value  $b_{cr}$ , i.e., almost in the entire existence domain [see Fig. 2(d)]. In row (c) of Fig. 3 we have plotted, for the sake of illustration, the initial and the final (after 500 propagation units) intensity distributions of a stable lattice vortex soliton. Comparing to the soliton molecules investigated in bulk nonlinear media, which were

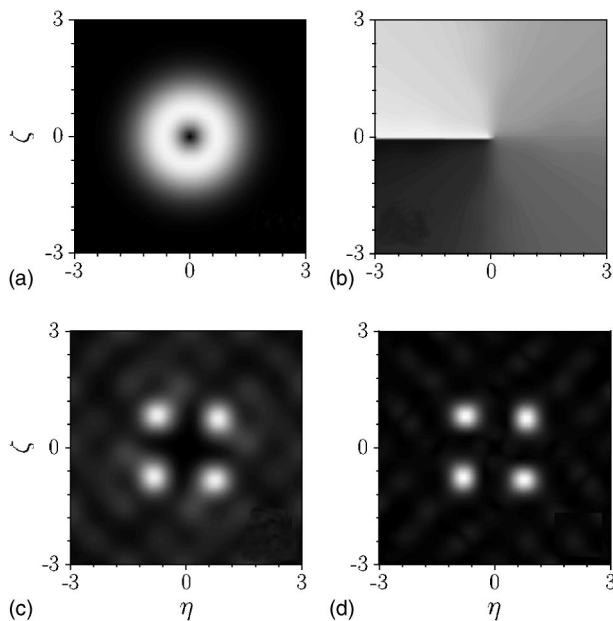


FIG. 5. Generation of the vortex solitons with only FF input. (a) Field and (b) phase distributions of the input FF beam with topological charge  $m_1=1$ . (c) FF beam and (d) SH beam at  $\xi=15$ . Lattice depth  $p=8$ , phase mismatch  $\beta=0$ .

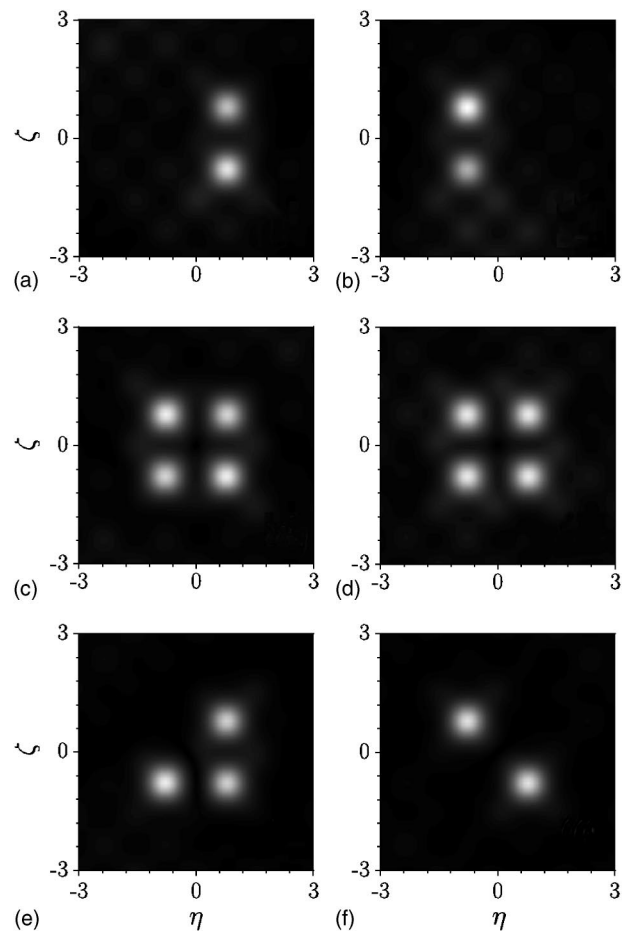


FIG. 6. Soliton algebra. The output soliton distribution depends on the topological charges  $m_1$  of FF wave and  $m_2$  of SH wave, respectively. In all cases,  $m_1=1$ . In (a)–(d), the amplitude of FF wave  $A=20$  and the amplitude of SH wave  $B=2$ . In (e) and (f)  $A=20$  and  $B=0.5$ . Plots (a)–(f) correspond the topological charges  $m_2=1, 3, 4, 6, 7, 8$ , respectively, and show the output SH field distribution at  $\xi=100$ . Lattice depth  $p=8$ , phase mismatch  $\beta=0$ .

shown to be *metastable* physical objects under suitable conditions, we conclude that, as expected on physical grounds, the effect of the two-dimensional lattice is to arrest the rotation of the soliton molecule and thus to assure the complete stabilization of the soliton complex. Since lattice causes strong azimuthal modulation of the vortex soliton, lattice removal results in complete soliton decay into four filaments, as shown in Fig. 4. Escape angles of filaments decrease with increase of input energy flow of vortex soliton.

To understand lattice vortex solitons generation from a radially symmetric input beam carrying a screw phase dislocation nested in the center and to show that different sets of output solitons can be obtained with different combinations of topological charges and shapes of the input beams we performed a comprehensive set of simulations of Eq. (1) with the input conditions corresponding to Gaussian beams with a phase dislocation nested in the center:

$$q_1(\xi=0, r, \varphi) = Ar^{|m_1|} \exp(im_1\varphi) \exp(-r^2/w_1^2),$$



$$q_2(\xi=0, r, \varphi) = Br^{|m_2|} \exp(im_2\varphi) \exp(-r^2/w_2^2), \quad (5)$$

where  $r = (\eta^2 + \zeta^2)^{1/2}$  is the radius,  $\varphi$  is the azimuthal angle,  $A$  and  $B$  are amplitudes of FF and SH waves,  $w_1$  and  $w_2$  are beam widths. Below we set the widths  $w_1 = w_2 = 1$  and suppose that topological charge of FF wave is given by  $m_1 = 1$ .

First, we consider nonseeded vortex soliton generation at  $B=0$ . At low input powers both input FF wave and generated SH wave exhibit complete diffraction, and input beam energy is redistributed between many lattice sites. With the increase of input energy flow [i.e., by increasing  $A$  in Eqs. (5)] the generation of lattice vortex soliton with unit topological charge becomes possible as shown in Fig. 5. Lattice soliton generation is accompanied with energy radiation [Figs. 5(c) and 5(d)] but the ratio between radiative losses and the output soliton energy flow decreases with increase of input energy flow.

In the case of seeded SH generation ( $B \neq 0$  and  $B \ll A$ ), the output field distribution can be controlled by the input topological charge of SH wave. For  $m_1 = 1$  vortex soliton generation is possible only for the vorticity-matched case when  $m_2 = 2$ , while all other values of  $m_2$  correspond to formation of trivial-phase soliton distributions, whose structure is dictated by lattice symmetry and energy exchange between FF and SH waves at the initial stage of propagation. Some representative output distributions are shown in Fig. 6. These plots show that the concept of “soliton algebra,” previously explored in homogeneous media [36], does also apply in the

presence of lattices, offering interesting opportunities for controlling the soliton dynamics.

In summary, we have shown that periodic lattices imprinted in quadratic nonlinear media can support four-hump vortex solitons with unit topological charge that are stable provided that their propagation constant is above a certain critical value. Below this critical value we have identified two types of instabilities: (i) an exponential type of instability leading to the final decay and spread out of the solitons across the lattice, and (ii) an oscillatory-type instability leading to the transformation of the lattice vortex soliton into a fundamental soliton without internal vorticity. We investigated the generation of the multicolor lattice vortex soliton from Gaussian beams with nested phase dislocations. The possibility to generate different output lattice soliton patterns, with and without vorticity, by varying the topological charges and amplitudes of the input beams in seeded excitation configurations, has been discussed. The generation of a 2D periodic potential in quadratic nonlinear media is a challenging issue, even though fabrication of 1D lattices has been already achieved using techniques which might be extended to 2D geometries. Also, the results presented here might be relevant to suitable atomic-molecular Bose-Einstein condensates held in optical lattices.

This work was partially supported by the Generalitat de Catalunya, by the Institució Catalana de Recerca i Estudis Avançats (ICREA), and by the Spanish Government through Grant No. BFM2002-2861.

- 
- [1] Yu. S. Kivshar and G. P. Agrawal, *Optical Solitons: From Fibers to Photonic Crystals* (Academic, San Diego, 2003).
- [2] G. I. Stegeman, D. J. Hagan, and L. Torner, *Opt. Quantum Electron.* **28**, 1691 (1996).
- [3] A. V. Buryak, P. Di Trapani, D. V. Skryabin, and S. Trillo, *Phys. Rep.* **370**, 63 (2002).
- [4] For a review, see, e.g., M. S. Soskin and M. V. Vasanetsov, in *Progress in Optics*, edited by E. Wolf (Elsevier, Amsterdam, 2001), Vol. 42.
- [5] V. I. Kruglov and R. A. Vlasov, *Phys. Lett. A* **111**, 401 (1985); L. Torner and D. V. Petrov, *Electron. Lett.* **33**, 608 (1997); W. J. Firth and D. V. Skryabin, *Phys. Rev. Lett.* **79**, 2450 (1997); J. P. Torres, J. M. Soto-Crespo, L. Torner, and D. V. Petrov, *J. Opt. Soc. Am. B* **15**, 625 (1998).
- [6] V. Tikhonenko, J. Christou, and B. Luther-Daves, *J. Opt. Soc. Am. B* **12**, 2046 (1995); D. V. Petrov, L. Torner, J. Martorell, R. Vilaseca, J. P. Torres, and C. Cojocar, *Opt. Lett.* **23**, 1444 (1998); M. S. Bigelow, P. Zerom, and R. W. Boyd, *Phys. Rev. Lett.* **92**, 083902 (2004).
- [7] M. Quiroga-Teixeiro and H. Michinel, *J. Opt. Soc. Am. B* **14**, 2004 (1997); I. Towers, A. V. Buryak, R. A. Sammut, B. A. Malomed, L.-C. Crasovan, and D. Mihalache, *Phys. Lett. A* **288**, 292 (2001); B. A. Malomed, L.-C. Crasovan, and D. Mihalache, *Physica D* **161**, 187 (2002); D. Mihalache, D. Mazilu, L.-C. Crasovan, I. Towers, A. V. Buryak, B. A. Malomed, L. Torner, J. P. Torres, and F. Lederer, *Phys. Rev. Lett.* **88**, 073902 (2002); D. Mihalache, D. Mazilu, I. Towers, B. A. Malomed, and F. Lederer, *Phys. Rev. E* **67**, 056608 (2003); D. Mihalache, D. Mazilu, B. A. Malomed, and F. Lederer, *ibid.* **69**, 066614 (2004); *J. Opt. B: Quantum Semiclassical Opt.* **6**, S341 (2004).
- [8] D. N. Christodoulides and R. I. Joseph, *Opt. Lett.* **13**, 794 (1988).
- [9] D. N. Christodoulides, F. Lederer, and Y. Silberberg, *Nature (London)* **424**, 817 (2003).
- [10] O. Bang and P. D. Miller, *Opt. Lett.* **21**, 1105 (1996).
- [11] Y. V. Kartashov, L. Torner, and V. A. Vysloukh, *Opt. Lett.* **29**, 1102 (2004); Y. V. Kartashov, A. S. Zelenina, L. Torner, and V. A. Vysloukh, *ibid.* **29**, 766 (2004).
- [12] R. Scharf and A. R. Bishop, *Phys. Rev. E* **47**, 1375 (1993).
- [13] O. Cohen, T. Schwartz, J. W. Fleischer, M. Segev, and D. N. Christodoulides, *Phys. Rev. Lett.* **91**, 113901 (2003).
- [14] N. Efremidis, S. Sears, D. N. Christodoulides, J. Fleischer, and M. Segev, *Phys. Rev. E* **66**, 046602 (2002).
- [15] J. Fleischer, T. Carmon, M. Segev, N. Efremidis, and D. N. Christodoulides, *Phys. Rev. Lett.* **90**, 023902 (2003).
- [16] J. Fleischer, M. Segev, N. Efremidis, and D. N. Christodoulides, *Nature (London)* **422**, 147 (2003).
- [17] D. Neshev, E. Ostrovskaya, Y. Kivshar, and W. Krolikowski, *Opt. Lett.* **28**, 710 (2003).
- [18] Y. V. Kartashov, V. A. Vysloukh, and L. Torner, *Opt. Express* **12**, 2831 (2004).

- [19] B. A. Malomed and P. G. Kevrekidis, *Phys. Rev. E* **64**, 026601 (2001).
- [20] J. Yang and Z. Musslimani, *Opt. Lett.* **23**, 2094 (2003).
- [21] Z. Musslimani and J. Yang, *J. Opt. Soc. Am. B* **21**, 973 (2004).
- [22] D. N. Neshev, T. J. Alexander, E. A. Ostrovskaya, and Yu. S. Kivshar, *Phys. Rev. Lett.* **92**, 123903 (2004).
- [23] J. Fleischer, J. Bartal, O. Cohen, O. Manela, M. Segev, J. Hudock, and D. N. Christodoulides, *Phys. Rev. Lett.* **92**, 123904 (2004).
- [24] A. A. Sukhorukov, Y. S. Kivshar, O. Bang, and C. M. Soukoulis, *Phys. Rev. E* **63**, 016615 (2000).
- [25] O. Bang, P. L. Christiansen, and C. B. Clausen, *Phys. Rev. E* **56**, 7257 (1997).
- [26] T. Peschel, U. Peschel, and F. Lederer, *Phys. Rev. E* **57**, 1127 (1998).
- [27] A. Kobayakov, S. Darmanyan, T. Pertsch, and F. Lederer, *J. Opt. Soc. Am. B* **16**, 1737 (1999).
- [28] B. A. Malomed, P. G. Kevrekidis, D. J. Frantzeskakis, H. E. Nistazakis, and A. N. Yannacopoulos, *Phys. Rev. E* **65**, 056606 (2002).
- [29] Z. Y. Xu, Y. V. Kartashov, L.-C. Crasovan, D. Mihalache, and L. Torner, *Phys. Rev. E* **70**, 066618 (2004).
- [30] R. Iwanow, R. Schiek, G. I. Stegeman, T. Pertsch, F. Lederer, Y. Min, and W. Sohler, *Phys. Rev. Lett.* **93**, 113902 (2004).
- [31] Y. V. Kartashov, L. Torner, and V. A. Vysloukh, *Opt. Lett.* **29**, 1117 (2004); Y. V. Kartashov, V. A. Vysloukh, and L. Torner, *ibid.* **29**, 1399 (2004).
- [32] S. Carrasco, L. Torner, J. P. Torres, D. Artigas, E. Lopez-Lago, V. Couderc, and A. Barthelemy, *IEEE J. Quantum Electron.* **8**, 497 (2002).
- [33] M. Soljačić, S. Sears, and M. Segev, *Phys. Rev. Lett.* **81**, 4851 (1998); M. Soljačić and M. Segev, *Phys. Rev. E* **62**, 2810 (2000); *Phys. Rev. Lett.* **86**, 420 (2001).
- [34] A. S. Desyatnikov and Yu. S. Kivshar, *Phys. Rev. Lett.* **87**, 033901 (2001); **88**, 053901 (2002).
- [35] Y. V. Kartashov, G. Molina-Terriza, and L. Torner, *J. Opt. Soc. Am. B* **19**, 2682 (2002); Y. V. Kartashov, L.-C. Crasovan, D. Mihalache, and L. Torner, *Phys. Rev. Lett.* **89**, 273902 (2002); L.-C. Crasovan, Y. V. Kartashov, D. Mihalache, L. Torner, Y. S. Kivshar, and V. M. Perez-Garcia, *Phys. Rev. E* **67**, 046610 (2003); D. Mihalache, D. Mazilu, L.-C. Crasovan, B. A. Malomed, F. Lederer, and L. Torner, *ibid.* **68**, 046612 (2003); *J. Opt. B: Quantum Semiclassical Opt.* **6**, S333 (2004).
- [36] L. Torner, J. P. Torres, D. V. Petrov, and J. M. Soto-Crespo, *Opt. Quantum Electron.* **30**, 809 (1998); S. Minardi, G. Molina-Terriza, P. Di Trapani, J. P. Torres, and L. Torner, *Opt. Lett.* **26**, 1004 (2001).